HHS Public Access

Author manuscript

J Bone Miner Res. Author manuscript; available in PMC 2020 August 01.

Published in final edited form as:

J Bone Miner Res. 2019 August ; 34(8): 1531–1542. doi:10.1002/jbmr.3714.

A new understanding of the role of IL-1 in age-related intervertebral disc degeneration in a murine model

Deborah J. Gorth, ScM., **Irving M. Shapiro, Ph.D., BDS.**, **Makarand V. Risbud, Ph.D.**

Department of Orthopaedic Surgery and Graduate Program in Cell Biology and Regenerative Medicine, Thomas Jefferson University, Philadelphia, PA, U.S.A.

Abstract

Increased cytokine expression, in particular interleukin-1β (IL-1β), is considered a hallmark of intervertebral disc degeneration. However, the causative relationship between IL-1 and age-dependent degeneration has not been established. To investigate the role of IL-1 in driving age-related disc degeneration, we studied the spine phenotype of global IL-1α/β double knockout (IL-1KO) mice at 12 and 20 months. Multiplex ELISA analysis of blood revealed significant reductions in the concentrations of IFN-γ, IL-5, IL-15, TNF-α, IP-10, and a trend of reduced concentrations of IL-10, MIP-1α, KC/GRO, and IL-6. However, the circulating level of MIP-2, a neutrophil chemattractant, was increased in the IL-1KO. The alterations in systemic cytokine levels coincided with altered bone morphology—IL-1KO mice exhibited significantly thicker caudal cortical bone at 12-and 20-months. Despite these systemic inflammatory and bony changes, IL-1 deletion only minimally affected disc health. Both wild type and IL-1KO mice showed age-dependent disc degeneration. Unexpectedly, rather than protecting the animals from degeneration, the aging phenotype was more pronounced in IL-1KO animals: knockout mice evidenced significantly more degenerative changes in the annulus fibrosis (AF) together with alterations in collagen type and maturity. At 20-months, there were no changes in nucleus pulposus (NP) extracellular matrix composition or cellular marker expression; however, the IL-1KO NP cells occupied a smaller proportion of the NP compartment that those of wild type controls. Taken together, these results show that IL-1 deletion altered the systemic inflammatory environment and vertebral bone morphology. However, instead of protecting discs from age-related disc degeneration, global IL-1 deletion amplified the degenerative phenotype.

Keywords

Genetic animal models; aging; cytokines; collagen; Chondrocytes; intervertebral disc degeneration

To whom correspondence should be addressed: Dr. Makarand V. Risbud, Department of Orthopaedic Surgery, Sidney Kimmel Medical College, Thomas Jefferson University, Philadelphia PA, 19107. Tel: 215 955 1063; Fax 215 955 9159; makarand.risbud@jefferson.edu.

Authors' roles

Study design: DG, IS and MR. Study conduct, data collection, data analysis: DG. Data interpretation: DG, IS, and MR. Drafting manuscript: DG. Revising manuscript content: DG, MR, IS. Approving final version of manuscript: DG, MR, IS. DG and MR takes responsibility for the integrity of the data analysis.

Conflicts of Interest: None for all authors.

INTRODUCTION

Low back pain (LBP) is a widespread, costly, and complex medical condition. Over ten percent of the population is currently experiencing low back pain; approximately one quarter of adults report having back pain the previous month, and the number of affected individuals rises to over eighty percent when considering the population who sought care for LBP in the previous year (1–3). LBP is intricately correlated with the health of the intervertebral disc; a study reviewing the MRIs of patients with persistent LBP showed disc degeneration in 87% of the participants (4).

The healthy intervertebral disc comprises three distinct structures: an inner gelatinous glycosaminoglycan-rich nucleus pulposus (NP), a fibrocartilaginous annulus fibrosus (AF) that circumferentially encases the NP, and cartilaginous endplates (EP) that cap the NP and AF superiorly and inferiorly. As the disc degenerates with age or disease, the NP becomes more fibrotic, losing proteoglycan content and consequently the ability to bind water, compromising the mechanical properties of the motion segment (5–7). The vacuolated notochordal-derived NP cells die or transition to cells that exhibit the characteristics of hypertrophic chondrocytes (6,7). In addition to these cellular and extracellular matrix changes, inflammatory cytokine expression increases with increasing severity of disc degeneration (8). These cytokines promote disc degeneration by activating matrix metalloproteinases (MMPs), causing further extracellular matrix breakdown (9–11). Interleukin-1β (IL-1β) and tumor necrosis factor-α (TNF-α) are the most commonly studied inflammatory cytokines in conjunction with disc degeneration.

IL-1β and its structurally distinct but functionally similar family member IL-1α signal by binding to IL-1 receptor, inducing the expression of inflammatory genes in addition to increasing their own transcription creating a positive feedback loop (12). IL-1 signaling is tempered by endogenous expression of IL-1 receptor antagonist (IL-1ra), which competitively binds to IL-1 receptor (13). IL-1β and its receptor expression increase as severity of degeneration increases without a commensurate increase in IL-1ra, suggesting that activation of IL-1β signaling is correlated with intervertebral disc degeneration (14). In addition to its role in promoting extracellular matrix breakdown, IL-1β also interferes with aggrecan transcription and translation, further tipping the scales from anabolism to catabolism (14). However, it is interesting to note that IL-1β is expressed in the NP compartment as early as postnatal day 0, implying that this cytokine may have other physiological functions (15). Considering its potential role in promoting disc degeneration, targeting IL-1β signaling is current being explored to treat disc degeneration (16,17). Despite the existing literature suggesting its importance, the causative link between IL-1 signaling and age-dependent degeneration has not been clearly established.

To gain further understanding of the role of IL-1 in the progression of age-dependent disc degeneration, we performed an in-depth analysis of the spinal phenotype of a previously generated global IL-1α/IL-1β double knockout mouse at twelve and twenty months of age (18). Surprisingly, while both genotypes showed age-related disc degeneration, the absence of IL-1 appeared to enhance the age-dependent phenotype as opposed to ameliorate the effect of aging on the intervertebral disc. These results thus provide the first evidence that

activation of IL-1 signaling alone is not sufficient to drive age-dependent degenerative pathologies of the disc.

RESULTS

IL-1KO mice show a reduction in systemic levels of inflammatory makers

To investigate if loss of IL-1 results in decrease in circulatory levels of inflammatory markers, we used a multiplex ELISA assay platform from Mesoscale Discovery to measure circulating levels of cytokines in the blood. Analysis of 12-month and 20-month samples in both wild type (WT) and IL-1KO mice showed no age-related differences, so the samples were grouped together for the subsequent comparative analysis between genotypes. IL-1KO mice showed reduced plasma concentrations of the vast majority of cytokines assayed, with significant reductions in IFN-γ, IL-5, TNF-α, IL-15, and IP-10 (Fig. 1). Moreover, IL-10, MIP-1α, KC/GRO, and IL-4 all showed a trend of reduction in IL1KO mice compared to wild-type mice (Fig. 1). The plasma concentrations of IL-6, IL-2, and MCP-1 were nearly identical between the genotypes. On the other hand, there was a significant increase in the serum concentration of MIP-2 with a trend of increasing levels of IL-17 and IL-33 in IL1KO mice (Fig. 1). These results suggest that there was an overall reduction in the systemic levels of inflammatory markers in IL-1KO mice.

IL-1KO vertebrae show cortical thickening with limited trabecular changes

Micro-computed tomography (μCT) analysis showed that the exterior caudal cortical shell had similar morphology between WT and IL-1KO mice (Fig. 2A, A'). However, optical sectioning of the reconstructed images in both sagittal and transverse planes clearly showed a pronounced thickening of the cortical shell of the caudal vertebrae of the 20-month IL-1KO mice (Fig. 2 B-C'). This cortical phenotype was also present in the 12-month animals (Fig. S1 A-C'). The cortical shells of the 20- and 12-month-old lumbar vertebrae were thinner than the caudal levels, with no appreciable between the genotypes (Fig. 2 D-F' and Fig. S1 D-F'). Quantification confirmed that the IL-1KO mice had a significant increase in caudal cortical shell thickness at both 12 ($p = 0.0004$) and 20 months ($p < 0.0001$), but changes in the lumbar cortical bone were undetectable at both time points (Fig. S1G and Fig. 2G). Despite the robust change in caudal cortical bone thickness, the trabecular bone in both the caudal and lumbar vertebrae was similar between the genotypes at 20 months of age (Fig. 2 H-K). Interestingly, while the IL-1KO caudal bone volume/total volume (BV/TV) showed a small but significant increase, the IL-1KO lumbar vertebrae did not show a difference between the genotypes (Fig. 2H). The trabecular thickness (Tb.th) mirrored the BV/TV result showing a significant increase in the IL-1KO caudal levels and no change in thickness of the lumbar levels (Fig. 2I). Both the BV/TV and Tb.th values were higher in the caudal than the lumbar vertebrae in both the genotypes. The remaining trabecular bone parameters such as trabecular spacing (Tb.sp) and trabecular number (Tb.n) were constant between the genotypes (Fig. 2 J and K). The 12-month IL-1KO animals showed no changes in the lumbar parameters, but some trabecular changes in the caudal parameters (Fig. S1H-M). Trabecular thickness was increased in the IL-1KO 12-month caudal levels, and trabecular spacing showed a corresponding decrease (Fig. S1 I,J). Noteworthy, the disc height index (DHI) and disc height were not affected in IL-1KO animals at 20 months of

age, but the caudal IL-1KO animals showed a 75μm increase in disc height despite no change in DHI (Fig 2 L and M and Fig. S1 L and M).

IL-1KO mice do not evidence protection from age-dependent disc degeneration

To investigate if IL-1 signaling plays an important role in age-dependent disc degeneration *in vivo,* we performed an in-depth histological analysis of IL-1KO and WT mice at 12 and 20 months of age. To accurately represent the full spectrum of observed phenotype, both representative healthy and representative degenerated disc images from 20-month-old mice were displayed (Fig 3 A-H'). Safranin O/Fast green and hematoxylin staining of healthy lumbar discs showed comparable phenotypes between the IL-1KO mice and their wild type controls (Fig. 3 A, A'). The healthier lumbar discs of both genotypes exhibited a vacuolated cell band and abundant proteoglycan-rich matrix comprising the NP compartment (Fig. 3 B, B'). The junction between NP and AF compartments was well demarcated, and the AF comprised a well-organized collagenous lamellae interspersed with AF cells (Fig. 3 C, C'). The EP of healthy WT and IL-1KO discs showed various levels of ossification and vascular infiltration, however there were no discernable differences between the genotypes (Fig. D, D').

In the degenerated levels, the discrete NP cell band was replaced by dispersed clusters of chondrocyte-like cells scattered throughout the NP compartment (Fig. 1E-F') with evidence of clonal proliferation (arrow, Fig. 1F, F'). Moreover, in these degenerated levels, the proteoglycan-rich extracellular NP matrix of the healthy lumbar disc was replaced by conspicuous pericellular and inter-territorial proteoglycan matrix interspersed with varying levels of collagenous material, a hallmark of hypertrophic cartilage as well as tissue fibrosis (Fig. 1 F, F'). The distinction between the NP and AF compartment was diffuse in the degenerated levels (Fig. 1G, G'). The EP of both the WT and IL1KO degenerated discs showed chondrocytic cell proliferation and clefts delaminating from the NP and EP (arrows, Fig 1H, H'). Similar to 20-month-old animals, 12-month-old IL-1KO and WT mice showed comparable lumbar disc histology, except that the discs were overall healthier than the 20-month-old animals (Fig. S2 A-B').

The caudal discs of both genotypes also showed age-dependent degeneration. Unlike the lumbar discs, the caudal disc NP cells of both age groups were clustered in the center of the NP compartment, and did not show the distinctive cell band (Fig. S2 C-F'). The NP cells towards the periphery of the compartment were vacuolated while the central cells were more condensed around a few pockets of proteoglycan-rich matrix (arrows, Fig. S2 F, F'). In healthy discs, the NP/AF border in both genotypes remained distinct (Fig. S2 G, G'). Additionally the EPs of wild type and IL-1KO animals showed discrete EP consisting of a thin layer of chondrocytes overlying the bony EP (Fig. S2 H, H'). The degenerated examples from both genotypes again showed similar pathological features (Fig. S2 I-L').

There were no significant level-by-level differences observed (Fig. S3), so lumbar and caudal levels were each pooled for analysis to provide an overview of degeneration status of the lumbar and caudal spine. Likewise, no sex dependent differences in NP and AF grades were found regardless of the genotype, so the presented grading data includes both sexes equally represented between genotypes. At 12 months compared to wild type controls, the

distribution of Modified Thompson scores of the IL-1KO lumbar discs showed a reduction of completely healthy Grade 1 NP and AF and an increased incidence of more degenerated NP and AF, tissues with higher grade scores (Fig. 3I). While at 20 months, the distribution of Modified Thompson scores was overall worse than at 12 months for both NP and AF in both genotypes, there was a less pronounced difference in the grade distribution between the two genotypes (Fig. 3I). The caudal grade distributions followed the same trends as the lumbar distributions, with a more pronounced trend in the distribution of AF scores in the 20-month-old IL-1KO caudal discs toward grade 3 and 4 than wild type controls (Fig. 3J).

Figure 3K shows the average Modified Thompson scores for lumbar levels at 12 and 20 months. Both genotypes showed a significant ($p < 0.0001$) age-dependent reduction in NP and AF health (Fig. 3K). The lumbar discs of wild type and IL-1KO mice showed comparable age-dependent changes. Like the lumbar discs, the NP and AF of caudal discs showed age-related degeneration regardless of the genotype (Fig. 3L). While the distribution of average Modified Thompson scores of the NP was similar at both 12 and 20 months, surprisingly, the average of AF scores in the IL-1KO caudal discs was significantly worse ($p = 0.0267$) than the wild type controls 4 (Fig. 3L). The caudal AF of IL-1KO levels showed an amplified age-dependent reduction in health.

NP cells in IL-1KO mice preserve their molecular phenotype but occupy a smaller proportion of the NP.

To determine if deletion of IL-1 results in altered molecular phenotype, we analyzed the expression of validated NP phenotypic markers, carbonic anhydrase 3 (CA3) and glucose transporter 1 (GLUT1). NP cells showed a robust expression of both of the markers and the expression was restricted to the NP compartment; staining was comparable between the two genotypes (Fig. 4 A-B'). Additionally, GLUT1 signal was seen in the vasculature of the bony EP, as is expected due to its known expression in immune cells (Fig. 4 B and B') (19). Quantification of staining in NP compartments confirmed comparable expression and thus the phenotypic similarities of cells between the genotypes (Fig. 4 A'', B''). Since both genotypes showed a spectrum of degeneration (Fig. 3), we investigated whether the NP marker expression was sensitive to disease status and if it was influenced by the genotype. The staining for NP cell marker CA3 decreased as severity of degeneration increased in both IL-1KO and WT animals (Fig. 2C-E'). To determine if there were any changes in the cellularity and cell size due to absence of IL-1, we quantified these parameters. While the lumbar NP compartment of IL-1KO discs had similar cellularity as the wild type controls, the cell band in IL-1KO mice occupied a smaller area of the compartment ($p = 0.0388$) (Fig. 3G and H). Taken together, these results show that NP cells in IL-1KO mice preserved their phenotypic characteristics but occupy a smaller proportion of the NP.

IL-1KO mice show differences in AF collagens but preserve proteoglycan composition of the NP

To delineate if absence of IL-1 in the systemic and local tissue environment during the aging process resulted in better preservation of extracellular matrix quality, we analyzed the status of major extracellular matrix components of the disc. Picrosirius red staining and polarized microscopy were performed to determine the collagen content and fiber diameter of the

fibrillar collagens. Both caudal and lumbar discs showed strong collagen localization in the AF with a weak pericellular staining around the NP cells (Fig. 5 A-D'). Polarized light images exhibited strong birefringence, an indicator of collagen fiber maturity, and showed variation between genotypes with IL-1KO AF containing more mature fibers (Fig. 5 B, B') (20). This difference was not visible in the lumbar discs (Fig. 4 D, D'). To quantify this difference, the percent area occupied by green, yellow, or red fibers was evaluated to confirm the significant ($p \leq 0.05$) difference in caudal fiber distribution and no difference in lumbar fiber maturity (Fig. 5E, F). To determine if there were genotype-specific differences in the expression of major collagens of the disc, we studied localization of collagens I and II. Both collagen I and collagen II were primarily localized in the AF in a fibril-morphology in the caudal and lumbar discs of both IL-1KO and WT mice (Fig. 5 G-H' and J-K'). Quantification of collagen staining in the AF compartment showed no differences in the amount of collagen I, but a significant decrease in collagen II in both caudal and lumbar IL-1KO discs (Fig. 5 G-H" and J-K"). Additionally, we measured the expression of cartilage oligomeric matrix protein (COMP), which helps maintain the structural integrity of the collagen matrix, in the caudal levels. We observed a significant decrease in COMP content in the IL-1KO mice (Fig. 5 I-I").

In addition to the AF collagen composition, we studied the localization and integrity of aggrecan, a predominant proteoglycan of the disc. Immunofluorescent staining revealed that aggrecan (ACAN) and chondroitin sulfate (CS), the major glycosaminoglycan component of aggrecan were predominantly localized in the NP compartment; the pattern and level of expression were similar between the IL-1KO and WT mice (Fig. 6 A-B"). To investigate if aggrecan turnover is affected in the mutant mice, we stained disc sections for aggrecanase generated N-terminal neoepitope ARG (ARGxx) of aggrecan; the staining was predominantly localized in the pericellular region in the AF with no changes between genotypes. In contrast to ARGxx, MMP generated N-terminal neoepitope DIPEN showed diffuse staining throughout the NP, but again there were no apparent differences between the two genotypes (Fig. 6 C-D"). Additionally we looked at collagen X staining, which is expressed during disc degeneration (6). Collagen X showed little staining in relatively healthy 20-month old discs (data not shown), however its expression was diffused throughout the NP of degenerated discs with strong pericellular staining around the NP cells that acquired hypertrophic chondrocyte-like morphology (Fig. 6 E-E"). These results show that the NP matrix content and composition were not affected in IL-1KO mice.

DISCUSSION

There is a vast body of literature that has linked inflammation and in particular IL-1β to disc disease (21–24). Studies of spinal phenotype of the global IL-1α/β double knockout were therefore undertaken with an aim to establish a causative relationship between this important cytokine and disc degeneration. We tested the hypothesis that activation of IL-1 signaling with aging contributes to age-dependent disc degeneration with the expectation that deletion of IL-1 is protective and results in better preservation of the tissue structure than in wild type mice. However, surprisingly, the results suggest that there was an overall lack of protection from age-related disc degeneration in the IL-1KO mice, though the IL-1KO mice fared worse on some criteria. The IL-1KO and wild type animals evidenced different vertebral

bone parameters and blood cytokine profiles. Knocking out IL-1 resulted in significant changes in the circulating cytokine profile with reductions in several key inflammatory cytokines including IFN-γ, TNF-α, IL-5, IL-15, and IP10. Previous studies have examined the cytokine profile of IL-1KO mice in response to an inflammatory stimulus; the cytokine-mediated inflammatory response is muted in these IL-1KO mice (25). While the IL-1KO mice in this study were not subjected to any acute stimulus to induce inflammation, aging itself creates a proinflammatory state (26). It was interesting to note that unlike other cytokines, MIP-2 was increased in the knockout mice. MIP-2 is secreted by cells to recruit lymphocytes (27) and it is plausible that in IL-1KO mice, the peripheral tissues secrete excess MIP-2 to compensate for the reduced immune function associated with decreased TNF-α and IFN-γ (28,29) Thus, in agreement with previous studies, the overall reduction in cytokines observed herein could be representative of a reduction in the systemic inflammatory state of IL-1KO mice.

In addition to the altered systemic cytokine profile, the lack of IL-1 resulted in alterations in vertebral bone morphology in the knockout mice characterized by marked cortical thickening in the caudal levels. The lack of detectable difference in the lumbar cortical bone is not surprising. Due to the 16 μm voxel size used for scanning and the average lumbar cortical thickness of 50 μm, a 20 percent difference between genotypes, observed in the caudal cortical bone, falls within the observational error for this measurement in the lumbar spine. The thicker cortical bone is likely due to reduced osteoclast function; the difference between genotypes was more pronounced in the 20-month-old mice than the 12-month-old mice, suggesting a possible catabolic mediated process as opposed to a developmental defect. Both the BV/TV and trabecular thickness showed an increase in the caudal vertebrae of the IL-1KO mice compared to WT controls at 20 months of age. While 12-month-old IL-1KO mice showed trends of increased BV/TV, only the change in trabecular thickness was significant. These results are in agreement with previous studies that showed increased cortical bone thickness in the long bones of these IL-1KO mice due to reduced osteoclast function (30,31).

It is noteworthy that despite the robust and significant changes in both systemic cytokine profile and vertebral bone phenotype, the NP of IL-1KO mice were not drastically affected. Very recent work suggests that the intervertebral disc is isolated from systemic inflammatory factors and alterations in neighboring vertebral bone morphology (32). While the NP cell molecular phenotype was preserved in IL-1KO mice, there was a small reduction in the area that cells occupied in IL-1KO lumbar levels. Since there was no apparent change in the pericellular matrix content or the cell number between the genotypes, this could imply that IL-1KO NP cells are smaller than WT NP cells. Smaller chondrocyte-like cells are associated with aging and degeneration (6). This result is consistent with a recent study showing that overexpressing inflammatory cytokine TNF−α leads to increased cell band size and a vacuolar morphology of NP cells (32). However, contrary to the current understanding of the role of cytokines in disc degeneration, the absence of IL-1 amplified the age-related degeneration in the caudal spine; the 20-month-old AF grades in IL-1KO mice were significantly worse than WT controls. The lack of phenotype in the lumbar AF compared to the caudal AF could arise from the difference in mechanical stress experienced by these sections of the axial skeleton (33). Increased displacement in the caudal spine translates to

elevated stress on the caudal discs, and knocking out IL-1 may impair the homeostatic ability of the AF to heal resulting micro fractures. The worse AF grades and reduced AF collagen II and COMP levels in the IL-1KO mice fits well with the important role that cytokines play in healing collagenous structures (34). This could indicate that systemic IL-1 signaling may be important to maintaining AF integrity and preventing herniation. IL-1 receptor type I (IL-1R) KO mice show reduced fibrosis in response to injury, consequently impaired collagen deposition could affect AF health in IL-1KO mice (35). An aging model of osteoarthritis showed the protective role of inflammatory cytokines in tissue degeneration; IL-6 knockout mice are more susceptible to age-related osteoarthritis, supporting the possible protective role of traditionally inflammatory cytokines in age-related tissue degeneration (36). Importantly, the observation that the caudal discs of IL-1KO mice possessed a higher content of mature collagen fibers and a corresponding decrease in thin, more nascent fibers, along with reduced collagen II levels was a clear reflection of the contribution of IL-1 to collagen homeostasis of the compartment. A recent study showed that IL-1β concentration in the disc is not age dependent (37). These observations underscore the complex interaction of the IL-1 genotype with the mechanical environment of the tissue, while at the same time providing the first evidence that IL-1 may have important physiological functions in the disc.

While our results initially appear to contradict a previous study of IL-1ra deficient mice that exhibit features consistent with early onset disc degeneration, there are several possibilities that could account for this difference. There is an inherent difference between removing an inhibitor of a positive feedback loop and removing one component of a redundant system promoting inflammation. Moreover, due to the inherent inter- and intra-animal variation, the smaller sample size used in the IL-1ra knockout mouse paper is more prone to this bias than the analysis of 32 caudal and 32 lumbar levels from 8 mice per genotype at each of the time-points in this present study (21). It is noteworthy that the cartilage degeneration and arthritic phenotype associated with IL-1ra knockout is highly strain dependent. The previous study of disc phenotype in IL-1ra knockouts was done on a BALB/c background while the work presented herein uses C57BL/6 mice (21). BALB/c mice deficient in IL-1ra spontaneously develop chronic inflammatory arthritis while IL-1ra deficient DBA/1 and B10.DR1 mice do not (38). The IL-1ra knockout driven arthritic phenotype was found to be dependent on a non-MHC genetic basis; by crossing the BALB/c and DBA/1 mice, and performing quantitative trail locus analysis, a region on chromosome 1 has been identified that contains the arthritis predisposing factor, and further genomic analysis indicates that it is likely interferon activated gene 204 (Ifi204) (39,40). This Ifi204 effect appears to be immune cell related; concurrently knocking out IL-17, a T cell-derived inflammatory cytokine, abrogated the development of arthritis in IL-1Ra KO (41). The analysis presented herein showed no significant change in systemic IL-17 between the genotypes, suggesting that an IL-17 mediated process would not affect these mice. It is therefore highly plausible that the genetic differences between the strains C57BL/6 (IL-1KO model) and BALB/c (IL-1ra KO) account for the observed differences (42). It is also important to acknowledge that the intervertebral disc is an immune privileged compartment, so an effect mediated by the involvement of T-cells may spare this organ while affecting the more accessible synovia of diarthrodial joints, an idea that is supported by the recent studies of hTNF-Tg mice (32). Taken together, IL-1

deletion altered the systemic inflammatory environment and vertebral bone morphology but did not have the expected effect on intervertebral disc health. Instead of protecting discs from age-related degeneration, global IL-1 deletion amplified the degenerative phenotype. This observation challenges the existing dogma that IL-1 expression in the disc is inherently pathological and raises the question, what are the physiological functions of this cytokine in the homeostasis of the disc compartment with aging.

MATERIALS AND METHODS

Mice –

All animal care procedures, housing, breeding, and the collection of animal tissues were performed in accordance with a protocol approved by the Institutional Animal Care and Use Committee (IACUC) of Thomas Jefferson University. The global IL-1α/β double knockout mice on C57BL/6 background generated by Horai et al. were used in this study (18). These mice harbor deletions of the part of exon 5 and intron 5 that encodes the N-terminal coding region for mature IL-1α and exons 3 through 5 that contain N-terminal coding region for mature IL-1β. These mice do not exhibit any mRNA expression of IL-1α and IL-1β confirming complete disruption of the IL-1 genes (18). Both male and female mice were used in these studies.

Blood collection and analysis –

Blood from both 12- (n=6) and 20- (n=6) month-old mice was collected immediately post-mortem by intra-cardiac puncture using heparinized needles. Red blood cells were separated using centrifugation. Cytokine concentrations were assayed using the V-PLEX Mouse Cytokine 19-Plex Kit (Meso Scale Diagnostics) according to manufacturer's specifications.

Micro-computed tomography analysis –

Micro-computed tomography scans (MicroCT40, SCANCO Medical, Switzerland) were performed on the lumbar and caudal IL1KO and wild type spines fixed with 4% PFA. Six mice per genotype were used and data was averaged as a mean of 2–3 spinal levels; all levels were plotted. Segments were scanned with an energy of 70 kVp, a current of 114 mA, and a 200-ms integration time producing a resolution of 16 mm^3 voxel size. The region of interest for analysis included the entire vertebral trabecular bone excluding cortical bone and the growth plate. Three-dimensional reconstructions of these trabecular bone scans were compiled using a Gaussian filter (σ = 1.0, support = 1) and converted to binary images with a fixed grey-scale threshold of 200. The data sets were then assessed using software supplied by the system manufacturer. To measure cortical thickness, spines were first aligned in the x-y plane using bony landmarks. Mean cortical thickness at the midpoint of each vertebra was manually quantified by averaging measurements at four points separated by 90 degrees (43). Disc height index (DHI) was calculated by dividing average disc height by the height of adjacent vertebral bodies.

Histological analysis –

Spines were decalcified in 20% ethylenediaminetetracetic acid (EDTA) at 4~C for 15 days before paraffin embedding. Mid-coronal 7 μm sections were used for staining. Xylene

deparaffinization followed by graded ethanol rehydration preceded all protocols. Safranin O/Fast Green/Hematoxylin stained slides were imaged using an Axio Imager 2 microscope, 5x/0.15 N-Achroplan or 10x/0,3 EC Plan-Neofluar objectives, Axiocam 105 color camera,and Zen2TM software (Carl Zeiss). Five blinded observers performed the scoring using a modified Thompson grading scale (44,45). Eight mice per genotype with 4 discs per mouse for both caudal and lumbar levels were analyzed.

Picrosirius Red™ Analysis –

Picrosirius Red™ staining visualized localization and quality of the collagen fibrils (20,46). Stained sections were imaged on a polarizing microscope (Eclipse LV100 POL, Nikon) (6). High magnification AF images were used for the analysis of the area occupied by green, yellow, or red pixels. Threshold levels for the colors remained constant.

Cell number quantification –

DAPI (Thermo Fisher Scientific, P36934) stained mid-coronal 7μm sections were used to quantify cell number in the NP. Three sections per animal (n=8) were used, and the NP area was used for analysis. Using ImageJ software (NIH), images were converted to 32-bit, then the background was subtracted using rolling=50. Next the images were auto-thresholded, made binary, and then cell number was calculated using the analyze particles function (47). Cell band percent area was calculated by hand contouring the cell band and NP compartment on safranin o/fast green/hematoxylin stained slides using ImageJ.

Immunofluorescence microscopy –

Mid-coronal 7 μm sections were used for all immunofluorescence studies. Sections were de-paraffinized and rehydrated as described above before antigen retrieval. Antigen retrieval was accomplished in an antibody-specific manner by either heated citrate buffer for 20 min or proteinase K for 10 min at room temperature or Chondroitinase ABC for 30 min at 37 °C, or TRIS/EDTA. Sections were blocked in 5% normal serum (Thermo Fisher Scientific, 10000C) in PBS-T (0.4% Triton X-100 in PBS), and incubated with primary antibody. The primary antibodies used were Aggrecan (1:50, Millipore, AB1031), Collagen I (1:100, Abcam, ab34710), Collagen II (1:400, Fitzgerald, 70R-CR008), COMP (1:200, Abcam, ab231977), CA3 (1:150, Santa Cruz, sc-50715), in blocking buffer at 4 °C overnight. For GLUT-1 (1:200, Abcam, ab40084), ARGxx (1:200, Abcam, ab3773), CS (1:300, Abcam, ab11570), and DIPEN (1:500, mdbiosciences, 1042002) staining, Mouse on Mouse Kit (Vector laboratories, BMK-2202) was used for blocking and primary antibody incubation. Tissue sections were washed and incubated with the appropriate Alexa Fluor®−594 conjugated secondary antibody (Jackson ImmunoResearch), at a dilution of 1:700 for 1 h at room temperature in dark. The sections were washed again with PBS-T (0.4% Triton X-100 in PBS) and mounted with ProLong® Gold Antifade Mountant with DAPI (Thermo Fisher Scientific, P36934). All mounted slides were allowed to set overnight before visualization with Axio Imager 2 using 5x/0.15 N-Achroplan or 10x/0,3 EC Plan-Neofluar objectives, AxioCam MRm camera, and Zen2TM software (Carl Zeiss). Exposure settings remained constant for all genotypes. Staining percent area quantification of three levels from six animals of each genotype was performed using ImageJ software (NIH); thresholds remained constant for each antibody.

Statistics –

Eight animals per genotype per time point were used for analysis (n=8), and data are presented as mean ± SD. Differences between genotypes were analyzed using the Student's *t* test when only two groups were presented on graph, or one-way ANOVA with a Sidak's multiple comparison test between groups when more than two groups were presented. Four lumbar or tail levels per mouse were combined and averaged for both μCT and histological analysis. At least five independent blinded individuals performed histological grading. Significance between collagen fiber distributions was determined using a $\chi 2$ test. All statistical analyses were performed using Prism7 (GraphPad Software). $P \leq 0.05$ was considered statistically significant.

Supplementary Material

Refer to Web version on PubMed Central for supplementary material.

ACKNOWLEDGMENTS

This study was funded by the National Institute of Arthritis and Musculoskeletal and Skin Diseases (NIAMS) of the National Institutes of Health under Award Numbers AR055655, AR064733, T32 AR052273, and F30AR071256.

Funded by the NIAMS

REFERENCES

1. Hoy D, Bain C, Williams G, March L, Brooks P, Blyth F, et al. A systematic review of the global prevalence of low back pain. Arthritis Rheum. 2012 6;64(6):2028–37. [PubMed: 22231424]
2. Freburger JK, Holmes GM, Agans RP, Jackman AM, Darter JD, Wallace AS, et al. The rising prevalence of chronic low back pain. Arch Intern Med. 2009 2 9;169(3):251–8. [PubMed: 19204216]
3. Deyo RA, Mirza SK, Martin BI. Back Pain Prevalence and Visit Rates. Spine (Phila Pa 1976). 2006 11 1;31(23):2724–7. [PubMed: 17077742]
4. Arnbak B, Jensen TS, Egund N, Zejden A, Hørslev-Petersen K, Manniche C, et al. Prevalence of degenerative and spondyloarthritis-related magnetic resonance imaging findings in the spine and sacroiliac joints in patients with persistent low back pain. Eur Radiol. 2015 7 22;26(4):1191–203. [PubMed: 26194456]
5. Silagi ES, Shapiro IM, Risbud MV Glycosaminoglycan synthesis in the nucleus pulposus: Dysregulation and the pathogenesis of disc degeneration. Matrix Biol. 2018 10;71–72:368–79.
6. Choi H, Tessier S, Silagi ES, Kyada R, Yousefi F, Pleshko N, et al. A novel mouse model of intervertebral disc degeneration shows altered cell fate and matrix homeostasis. Matrix Biol. 2018 3 29;70:102–22. [PubMed: 29605718]
7. Zhang Y, Xiong C, Kudelko M, Li Y, Wang C, Wong YL, et al. Early onset of disc degeneration in SM/J mice is associated with changes in ion transport systems and fibrotic events. Matrix Biol. 2018;70:123–39. [PubMed: 29649547]
8. Le Maitre CL, Hoyland JA, Freemont AJ. Catabolic cytokine expression in degenerate and herniated human intervertebral discs: IL-1beta and TNFalpha expression profile. Arthritis Res Ther. 2007 1;9(4):R77. [PubMed: 17688691]
9. Johnson ZI, Doolittle AC, Snuggs JW, Shapiro IM, Le Maitre CL, Risbud MV. TNF-α promotes nuclear enrichment of the transcription factor TonEBP/NFAT5 to selectively control inflammatory but not osmoregulatory responses in nucleus pulposus cells. J Biol Chem. 2017 10 20;292(42): 17561–75. [PubMed: 28842479]
10. Wang X, Wang H, Yang H, Li J, Cai Q, Shapiro IM, et al. Tumor Necrosis Factor-α- and Interleukin-1β-Dependent Matrix Metalloproteinase-3 Expression in Nucleus Pulposus Cells

Requires Cooperative Signaling via Syndecan 4 and Mitogen-Activated Protein Kinase-Nuclear Factor κB Axis: Implications in Inflammatory D. Am J Pathol. 2014 7 22;184(9):1–13.

11. Wang J, Tian Y, Phillips KLE, Chiverton N, Haddock G, Bunning RA, et al. Tumor necrosis factor α- and interleukin-1β-dependent induction of CCL3 expression by nucleus pulposus cells promotes macrophage migration through CCR1. Arthritis Rheum. 2013 3;65(3):832–42. [PubMed: 23233369]
12. Weber A, Wasiliew P, Kracht M. Interleukin-1 (IL-1) Pathway. Sci Signal. 2010 1 19;3(105):cm1-cm1.
13. Schreuder H, Tardif C, Trump-Kallmeyer S, Soffientini A, Sarubbi E, Akeson A, et al. A new cytokine-receptor binding mode revealed by the crystal structure of the IL-1 receptor with an antagonist. Nature. 1997 3 13;386(6621):194–200. [PubMed: 9062194]
14. Le Maitre CL, Freemont AJ, Hoyland JA. The role of interleukin-1 in the pathogenesis of human intervertebral disc degeneration. Arthritis Res Ther. 2005 1;7(4):R732–45. [PubMed: 15987475]
15. Peck SH, McKee KK, Tobias JW, Malhotra NR, Harfe BD, Smith LJ. Whole Transcriptome Analysis of Notochord-Derived Cells during Embryonic Formation of the Nucleus Pulposus. Sci Rep. 2017 12 5;7(1):10504. [PubMed: 28874804]
16. Gorth DJ, Mauck RL, Chiaro JA, Mohanraj B, Hebela NM, Dodge GR, et al. IL-1ra delivered from poly(lactic-co-glycolic acid) microspheres attenuates IL-1beta mediated degradation of nucleus pulposus in vitro. Arthritis Research & Therapy. 2012 p. R179. [PubMed: 22863285]
17. Gorth DJ, Martin JT, Dodge GR, Elliott DM, Malhotra NR, Mauck RL, et al. In vivo retention and bioactivity of IL-1ra microspheres in the rat intervertebral disc: a preliminary investigation. J Exp Orthop. 2014 12;1(1):15. [PubMed: 26914760]
18. Horai R, Asano M, Sudo K, Kanuka H, Suzuki M, Nishihara M, et al. Production of mice deficient in genes for interleukin (IL)-1alpha, IL-1beta, IL-1alpha/beta, and IL-1 receptor antagonist shows that IL-1beta is crucial in turpentine-induced fever development and glucocorticoid secretion. J Exp Med.1998 5 4;187(9):1463–75. [PubMed: 9565638]
19. Maciver NJ, Jacobs SR, Wieman HL, Wofford JA, Coloff JL, Rathmell JC. Glucose metabolism in lymphocytes is a regulated process with significant effects on immune cell function and survival. J Leukoc Biol. 2008 10;84(4):949–57. [PubMed: 18577716]
20. Steplewski A, Fertala J, Beredjiklian PK, Abboud JA, Wang MLY, Namdari S, et al. Blocking collagen fibril formation in injured knees reduces flexion contracture in a rabbit model. J Orthop Res. 2017 5 1;35(5):1038–46. [PubMed: 27419365]
21. Phillips KLE, Jordan-Mahy N, Nicklin MJH, Le Maitre CL. Interleukin-1 receptor antagonist deficient mice provide insights into pathogenesis of human intervertebral disc degeneration. Ann Rheum Dis. 2013 11 1;72(11):1860–7. [PubMed: 23396662]
22. Phillips KLE, Cullen K, Chiverton N, Michael ALR, Cole AA, Breakwell LM, et al. Potential roles of cytokines and chemokines in human intervertebral disc degeneration: interleukin-1 is a master regulator of catabolic processes. Osteoarthritis Cartilage. 2015 7;23(7):1165–77. [PubMed: 25748081]
23. Johnson ZI, Schoepflin ZR, Choi H, Shapiro IM, Risbud MV. Disc in flames: Roles of TNF-α and IL-1β in intervertebral disc degeneration. Eur Cell Mater. 2015 9 21;30:104–16; discussion 116–7. [PubMed: 26388614]
24. Risbud MV, Shapiro IM. Role of cytokines in intervertebral disc degeneration: pain and disc content. Nat Rev Rheumatol. 2014 1 1;10(1):44–56. [PubMed: 24166242]
25. Fantuzzi G, Dinarello CA. The inflammatory response in interleukin-1β-deficient mice: comparison with other cytokine-related knock-out mice. J Leukoc Biol. 1996 4 1;59(4):489–93. [PubMed: 8613694]
26. Ferrucci L, Corsi A, Lauretani F, Bandinelli S, Bartali B, Taub DD, et al. The origins of age-related proinflammatory state. Blood. 2005 3 15;105(6):2294–9. [PubMed: 15572589]
27. Ohtsuka Y, Lee J, Stamm DS, Sanderson IR. MIP-2 secreted by epithelial cells increases neutrophil and lymphocyte recruitment in the mouse intestine. Gut. 2001 10;49(4):526–33. [PubMed: 11559650]

28. Lee E-Y, Schultz KLW, Griffin DE. Mice Deficient in Interferon-Gamma or Interferon-Gamma Receptor 1 Have Distinct Inflammatory Responses to Acute Viral Encephalomyelitis. Peterson KE, editor. PLoS One. 2013 10 24;8(10):e76412.
29. Pasparakis M, Alexopoulou L, Episkopou V, Kollias G. Immune and inflammatory responses in TNF alpha-deficient mice: a critical requirement for TNF alpha in the formation of primary B cell follicles, follicular dendritic cell networks and germinal centers, and in the maturation of the humoral immune response. J Exp Med. 1996 10 1;184(4):1397–411. [PubMed: 8879212]
30. Kim JH, Jin HM, Kim K, Song I, Youn BU, Matsuo K, et al. The Mechanism of Osteoclast Differentiation Induced by IL-1. J Immunol. 2009 8 1;183(3):1862–70. [PubMed: 19587010]
31. Lee Y-M, Fujikado N, Manaka H, Yasuda H, Iwakura Y. IL-1 plays an important role in the bone metabolism under physiological conditions. Int Immunol. 2010 10 1;22(10):805–16. [PubMed: 20679512]
32. Gorth DJ, Shapiro IM, Risbud MV. Transgenic mice overexpressing human TNF-α experience early onset spontaneous intervertebral disc herniation in the absence of overt degeneration. Cell Death Dis. 2019 1 18;10(1):7.
33. Sarver JJ, Elliott DM. Mechanical differences between lumbar and tail discs in the mouse. J Orthop Res. 2005 1 1;23(1):150–5. [PubMed: 15607887]
34. Lin TW, Cardenas L, Glaser DL, Soslowsky LJ. Tendon healing in interleukin-4 and interleukin-6 knockout mice. J Biomech. 2006 1 1;39(1):61–9. [PubMed: 16271588]
35. Thomay AA, Daley JM, Sabo E, Worth PJ, Shelton LJ, Harty MW, et al. Disruption of interleukin-1 signaling improves the quality of wound healing. Am J Pathol. 2009 6;174(6):2129–36. [PubMed: 19389930]
36. de Hooge ASK, van de Loo FAJ, Bennink MB, Arntz OJ, de Hooge P, van den Berg WB. Male IL-6 gene knock out mice developed more advanced osteoarthritis upon aging. Osteoarthr Cartil. 2005 1 1;13(1):66–73. [PubMed: 15639639]
37. Novais E-JM, Diekman BO, Shapiro IM, Risbud MV. p16Ink4a deletion in cells of the intervertebral disc affects their matrix homeostasis and senescence associated secretory phenotype without altering onset of senescence. Matrix Biol. Forthcoming 2019.
38. Zhou F, He X, Iwakura Y, Horai R, Stuart JM. Arthritis in mice that are deficient in interleukin-1 receptor antagonist is dependent on genetic background. Arthritis Rheum. 2005 12 1;52(12):3731–8. [PubMed: 16320323]
39. Cao Y, Liu X, Deng N, Jiao Y, Ma Y, Hasty KA, et al. Congenic Mice Provide Evidence for a Genetic Locus That Modulates Spontaneous Arthritis Caused by Deficiency of IL-1RA. Bobé P, editor. PLoS One. 2013 6 28;8(6):e68158.
40. Tian C, Liu X, Zhu X, Cao Y, Deng N, Hasty KA, et al. Ifi204 as the most favored candidate gene that regulates susceptibility to spontaneous arthritis in mice deficient in IL-1ra. Gene Reports. 2018 9 1;12:21–9.
41. Nakae S, Saijo S, Horai R, Sudo K, Mori S, Iwakura Y. IL-17 production from activated T cells is required for the spontaneous development of destructive arthritis in mice deficient in IL-1 receptor antagonist. Proc Natl Acad Sci. 2003 5 13;100(10):5986–90. [PubMed: 12721360]
42. Tsang S, Sun Z, Luke B, Stewart C, Lum N, Gregory M, et al. A comprehensive SNP-based genetic analysis of inbred mouse strains. Mamm Genome. 2005 7;16(7):476–80. [PubMed: 16151692]
43. Fox KM, Kimura S, Powell-Threets K, Plato CC. Radial and ulnar cortical thickness of the second metacarpal. J Bone Miner Res. 2009 12 3;10(12):1930–4.
44. Thompson JP, Pearce RH, Schechter MT, Adams ME, Tsang IK, Bishop PB. Preliminary evaluation of a scheme for grading the gross morphology of the human intervertebral disc. Spine (Phila Pa 1976). 1990 5;15(5):411–5. [PubMed: 2363069]
45. McCann MR, Patel P, Pest MA, Ratneswaran A, Lalli G, Beaucage KL, et al. Repeated exposure to high-frequency low-amplitude vibration induces degeneration of murine intervertebral discs and knee joints. Arthritis Rheumatol. 2015 5;67(8):2164–75. [PubMed: 25891852]
46. Whittaker P, Kloner RA, Boughner DR, Pickering JG. Quantitative assessment of myocardial collagen with picrosirius red staining and circularly polarized light. Basic Res Cardiol. 1994;89(5): 397–410. [PubMed: 7535519]

47. Schneider CA, Rasband WS, Eliceiri KW. NIH Image to ImageJ: 25 years of image analysis. Nat Methods. 2012 6 28;9(7):671–5. [PubMed: 22930834]

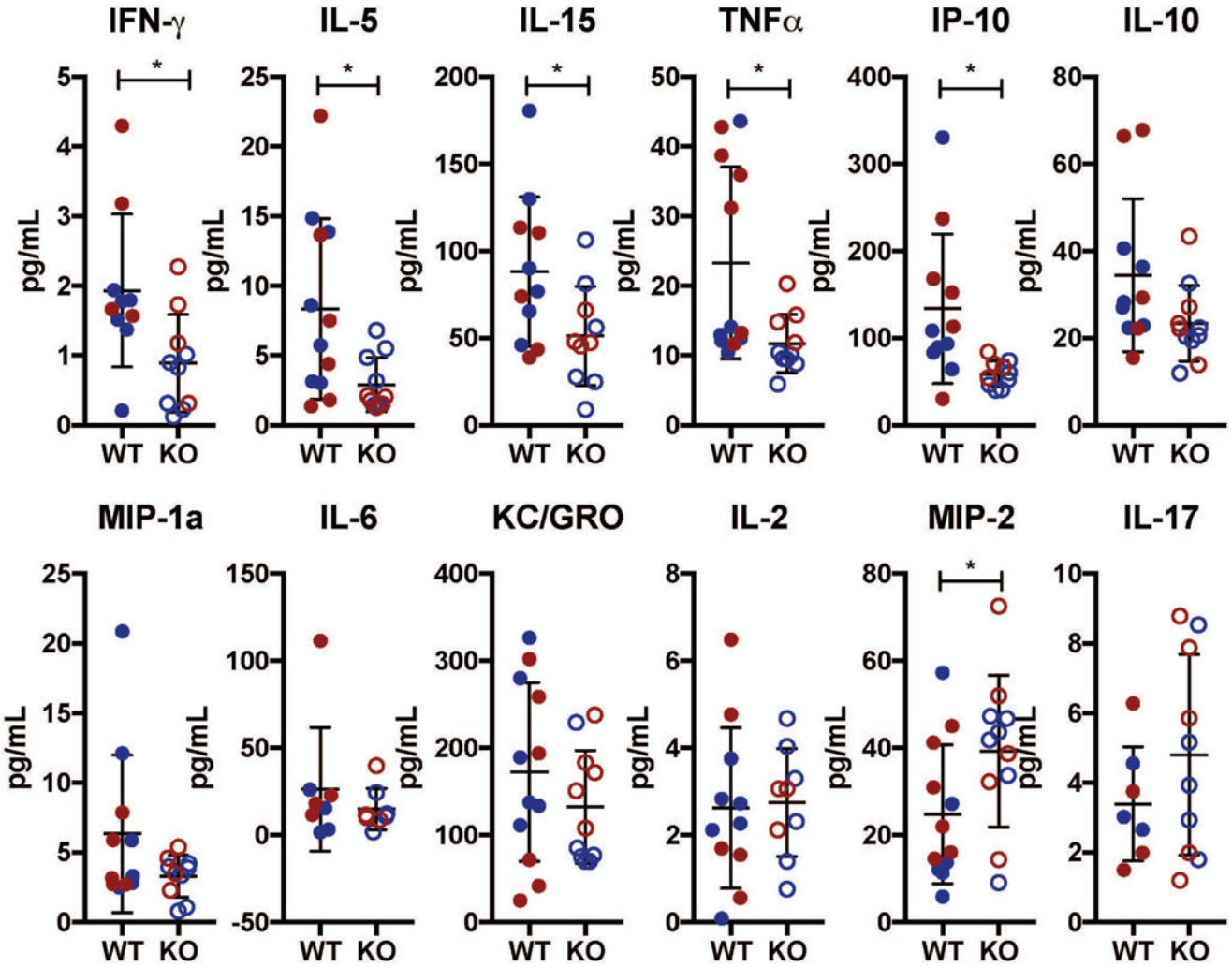

Figure 1: Blood cytokine levels in IL-1KO mice showed an overall decrease compared to wild-type mice.

Blood cytokine analysis of 12-month-old (shown in blue n=6) and 20-month-old (shown in red n=6) wild type (filled circle) and IL-1KO (open circle) mice. IFN-γ, IL-5, IL-15, TNF-α, and IP-10 showed a significant decrease in concentration in IL-1KO mice. IL-10, MIP-1α, KC/GRO, and IL-6 all showed a trend of decrease in the IL-1KO mice. IL-2 showed no change between the genotypes. MIP-2 showed a significant increase in concentration, while IL-17 showed a trend of increase in IL-1KO mice. Scatter plots show all data points and plotted as mean ±SD. t-test was used to determine significance between groups. * $p \leq 0.05$

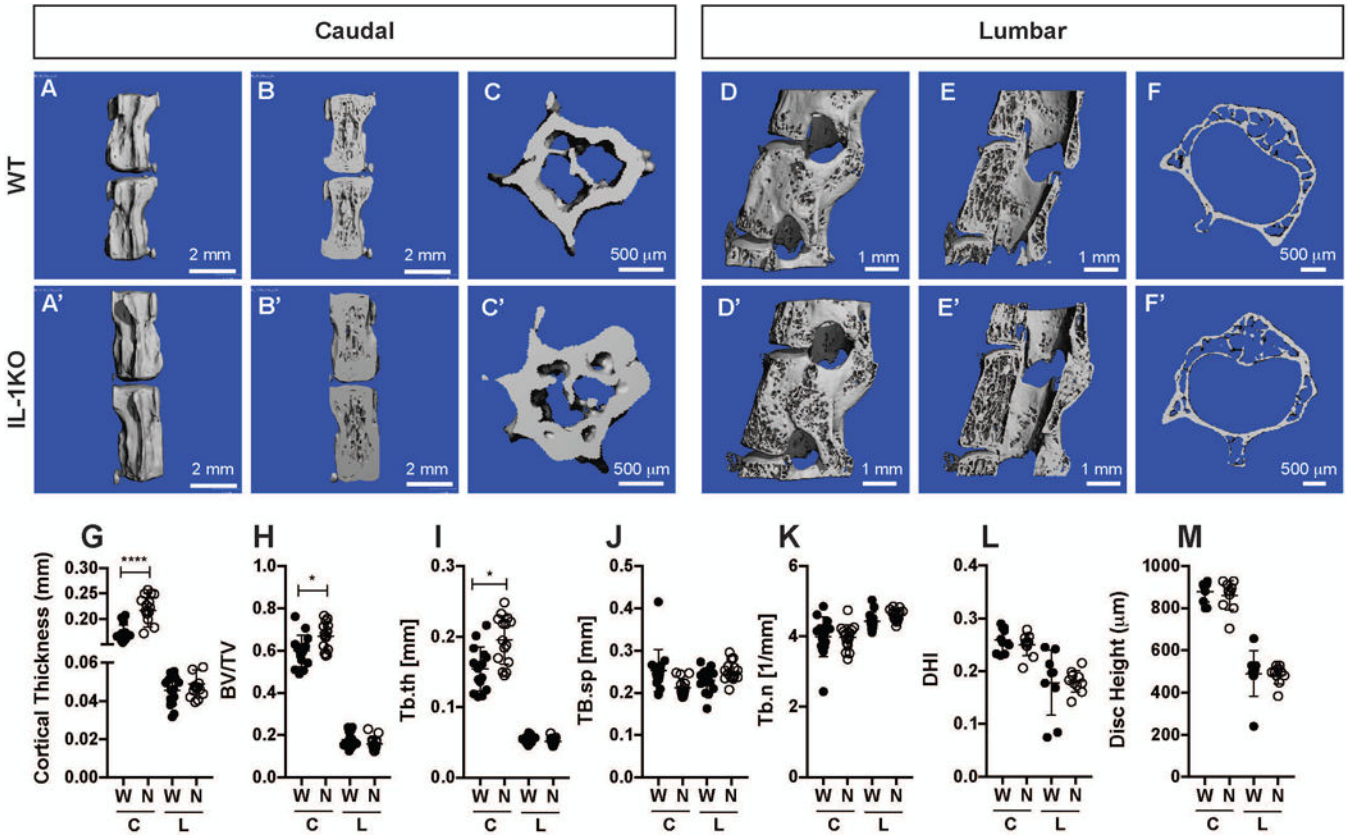

Figure 2: IL1KO vertebrae showed cortical thickening with limited trabecular changes.

(A-B') Representative µCT scans of caudal motion segments of 20-month-old spines showing cortical thickening. (C-C') Cross section of a representative 20-month-old vertebrae showing a robust cortical thickening. (D-F') Representative µCT scans 20-month-old lumbar vertebrae (D-D') whole, (E-E') optical hemi-section, and (F-F') cross section. (G) Quantification of cortical thickness in caudal and lumbar vertebrae of 20-month-old mice. (H-M) Bone volume/trabecular volume (BV/TV), trabecular thickness (Tb.th), trabecular spacing (Tb.s), trabecular number (Tb.n), disc height index (DHI), and disc height index of IL1KO and wild type mice (mean ±SD) (n = 6 mice per genotype with 3 consecutive vertebrae/animal). Scatter plots show all data points and plotted as mean ±SD. Significance was determined using ANOVA and Sidak's multiple comparison test. ns = not significant, * $p \leq 0.05$, **** $p \leq 0.0001$.

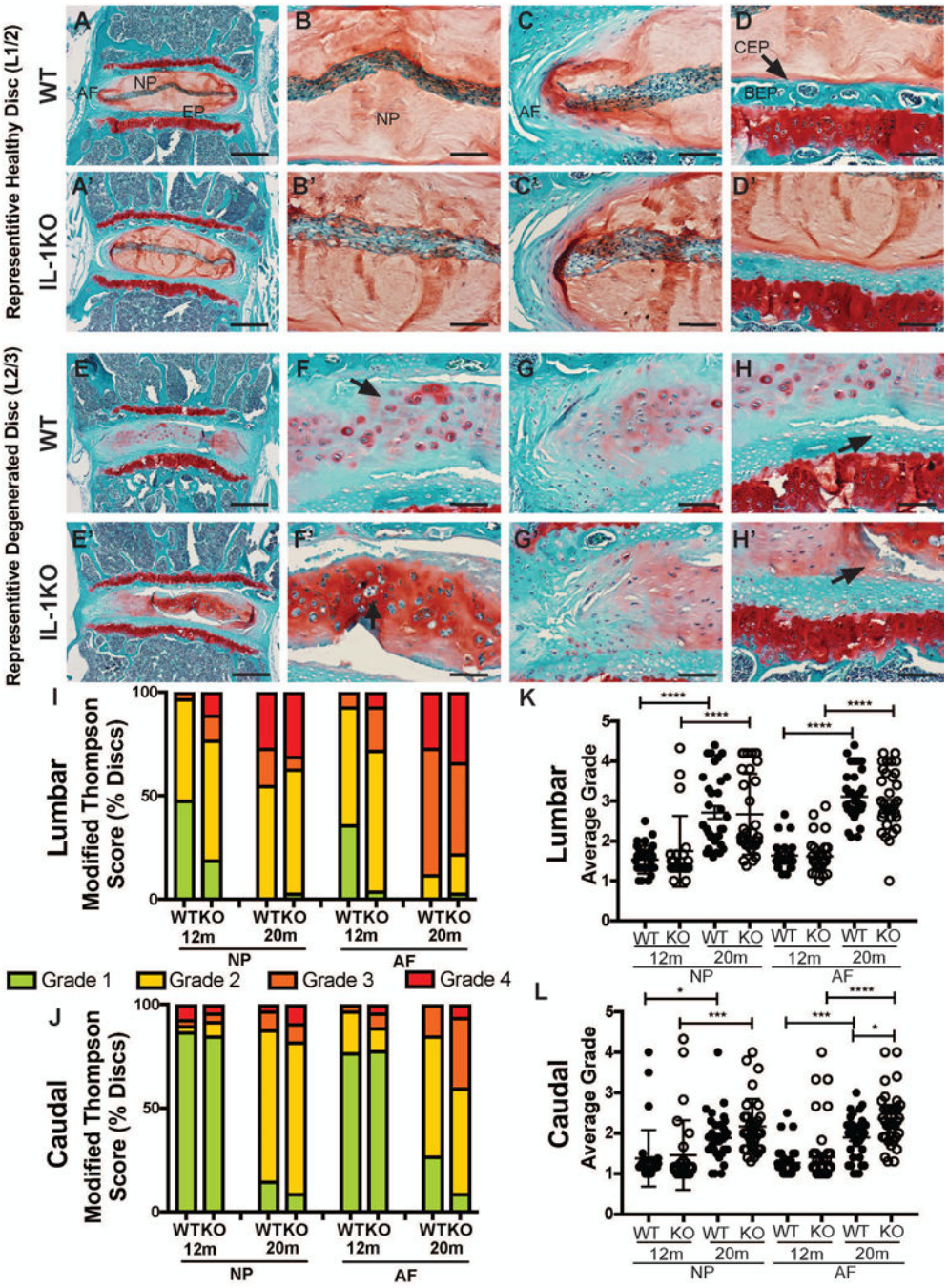

Figure 3: Both IL-1KO and wild type mice evidenced age dependent spectrum of degeneration.

(A-H') Safranin O/Fast Green/ Hematoxylin staining of coronal sections of wild type and IL-1KO mouse intervertebral discs showing both representative healthy discs (A-D') and representative degenerated levels (E-H') with the NP, AF, CEP, and BEP labeled on the top row for reference (left column, scale bars = 200μm; right three columns, scale bars = 50μm). (I, J) Distribution of histological grades of (I) lumbar and (J) caudal discs using the modified Thomson scale for 12-month-old and 20-month-old mice. (K, L) Average modified Thompson scores for (K) lumbar and (L) caudal intervertebral discs of 12-month and 20-

month-old WT and IL-1KO mice. Data was collected from 4 caudal and 4 lumbar discs per mouse (n=8 mice/genotype). Scatter plots show all data points and plotted as mean ±SD. Significance was determined using ANOVA and Sidak's multiple comparison test. * $p \leq 0.05$, *** $p \leq 0.001$, **** $p \leq 0.0001$.

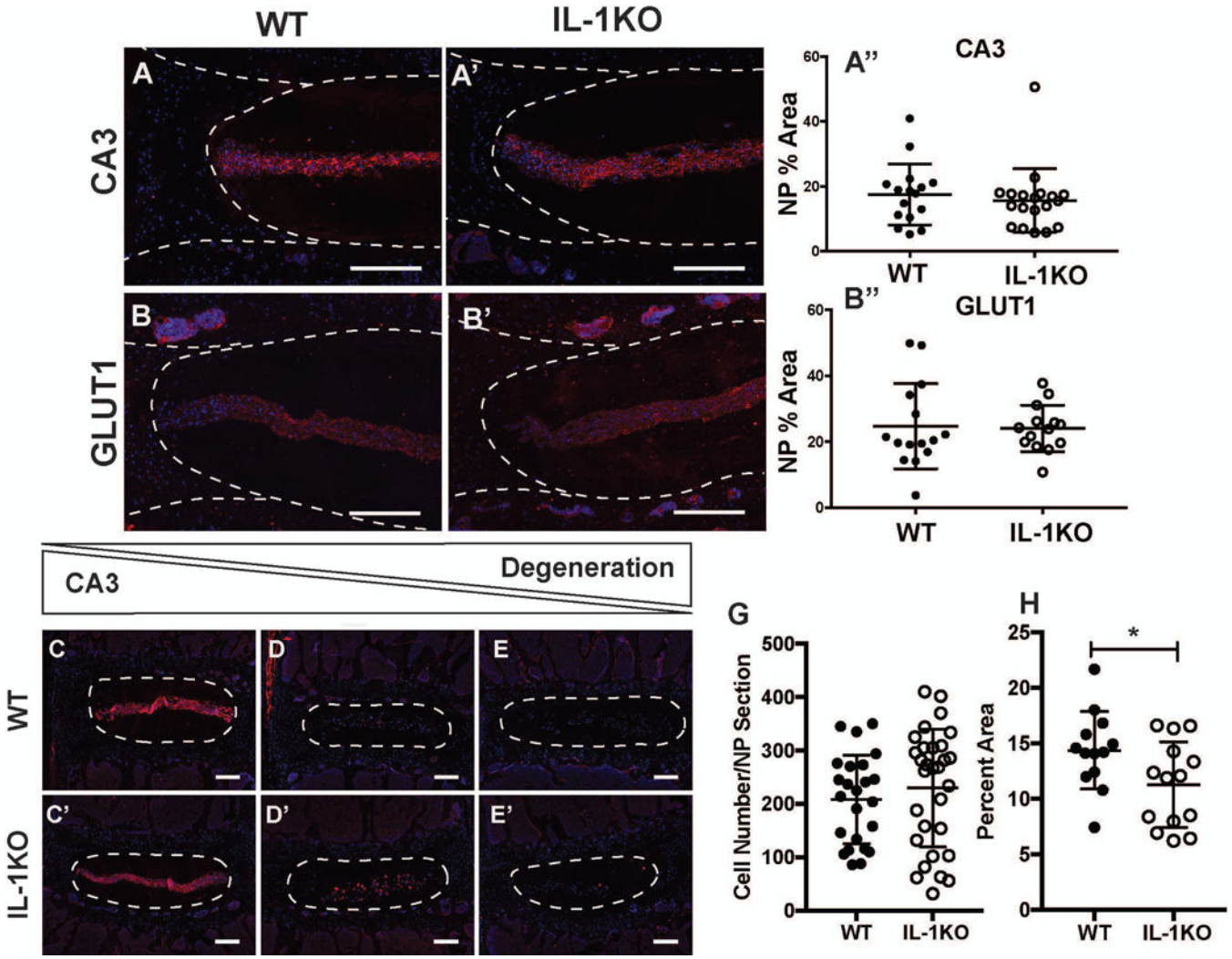

Figure 4: NP cells in IL-1KO mice were phenotypically similar to wild-type mice but occupied smaller proportion of the NP compartment.

(A,A') Representative images showed similar expression of NP cell markers carbonic anhydrase 3 (CA3) and (B,B') glucose transporter 1 (GLUT1) in WT and IL-1KO lumbar discs (scale bar = 200 μm). Quantification of NP markers from 3 levels from 6 animals each per genotype confirmed comparable expression of (A'') CA3 and (B'') GLUT1 between genotypes. (C, C') Expression of CA3 was robust in healthy lumbar levels and is reduced and nearly absent in increasingly degenerated discs (D-E') (Scale bar = 200 μm). (G) NP compartment showed comparable cell number between WT and IL-1KO mice. (H) The area occupied by the NP cell band in lumbar discs is significantly smaller in the IL-1KO animals. Quantitative data was plotted as mean ±SD and differences between groups were analyzed using t-test. * $p \leq 0.05$

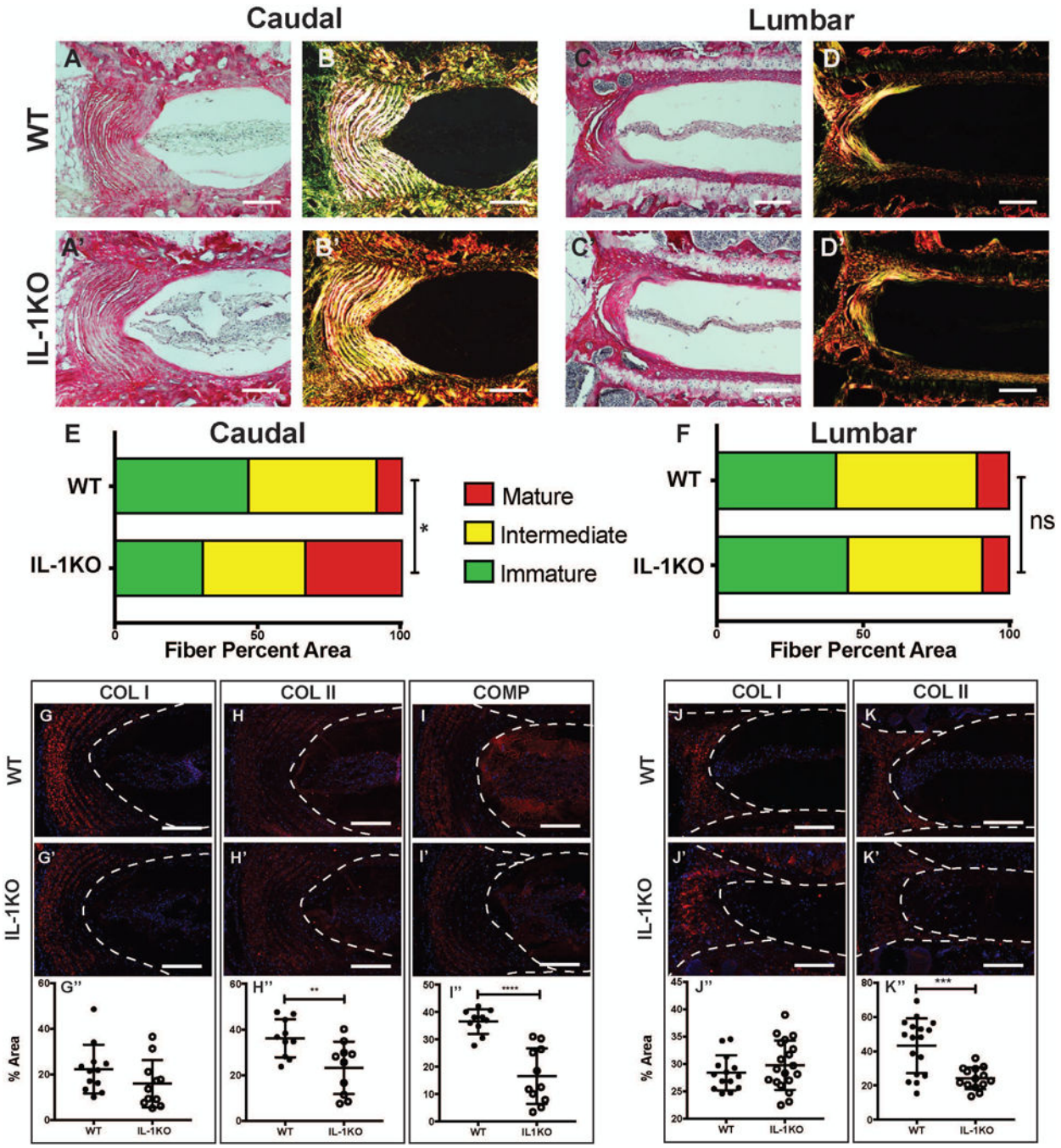

Figure 5: IL-1KO discs show differences in AF collagen content.

(A-D') Picrosirius red staining of 20-month-old (A-B') caudal and (C-D') lumbar discs showing collagen organization in the annulus fibrosus. Collagen fibers visualized under polarized light (B and D) show organized lamellae (scale bar 50 μm). (E, F) Quantification of the fiber content distribution in (E) caudal and (F) lumbar levels (n = 6 animals/genotype). Representative images of immunofluorescence staining of disc and quantification showed comparable expression of (G) caudal collagen I (COL I) with a reduction in (H) caudal collagen II (COL II) levels in AF compartment and (I) cartilage oligomeric matrix

protein (COMP) levels in the NP compartment of IL-1KO mice. (J) Col I and (K) Col II staining in the lumbar levels followed the trend as caudal levels. Staining was performed on 6 animals/genotype and 3 levels per animal; scale bar = 200μm. Significance between fiber distribution was determined using $\chi 2$ test and differences between immunofluorescence staining data plotted as mean ±SD was analyzed using t-test. * $p \leq 0.05$, *** $p \leq 0.001$, **** $p \leq 0.0001$

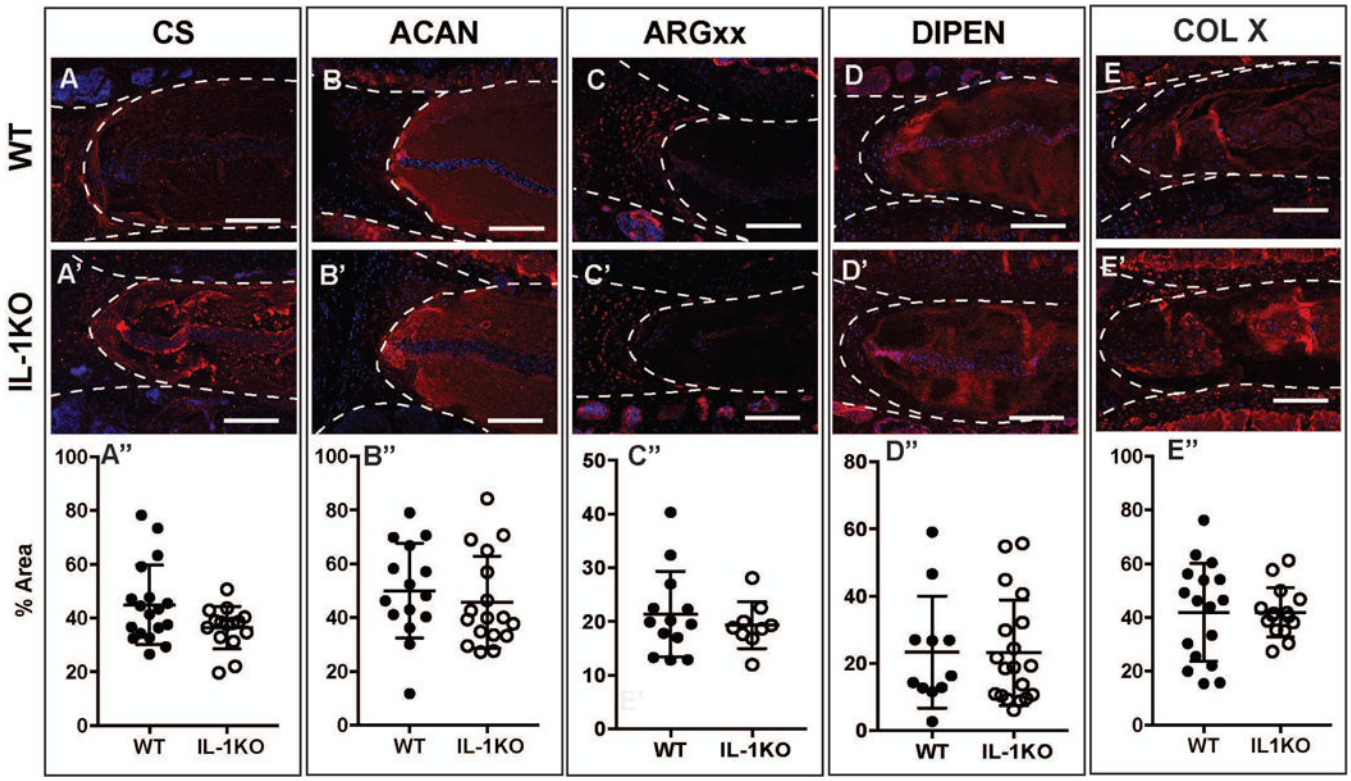

Figure 6: IL-1KO and WT mice showed comparable proteoglycan content and composition.

(A-E") Representative immunofluorescence staining images of discs from 20-month-old WT and IL-1KO mice and their quantification showed comparable expression levels of (A-A") Chondortin sulfate (CS), (B-B") aggrecan (ACAN) and aggrecan cleavage products (C-C") ARGxx, (D-D") DIPEN, and (E-E") collagen X done on degenerated levels. (n = 6 animals/genotype and 3 levels per animal; scale bar = 200 μm). Differences between immunofluorescence staining data plotted as mean ±SD and analyzed using t-test. No significant differences were found.